

EVALUATION OF FINITE ELEMENT BASED CORRECTION OF LAYER REMOVAL DURING XRD MEASUREMENTS FOR GEOMETRIES AND STRESS DISTRIBUTIONS OF INTEREST IN AIRCRAFT ENGINES

Yogesh K. Potdar¹, Karthick Chandraseker², Amit Kale¹, Rohinton Irani¹, Robert McClain³, Mike Hartle³, Paul Domas⁴

¹Mechanical Engineer (GE Global Research), ²Research Intern (GE Global Research),
³Sr. Staff Engineer and ⁴Consulting Engineer (GE-Aviation)

¹One Research Circle, K1-3C2B, NISKAYUNA, NY 12309, USA
¹potdar@research.ge.com

ABSTRACT

During X-Ray diffraction measurements of residual stresses, sub-surface stresses are measured after removing material layers by electro-polishing. The measured stresses are different from what they were initially before material layers were removed. The required corrections to calculate pre-removal stresses are significant when a thick layer of material is removed relative to the overall thickness of the part. Analytical correction formulae exist only for simple geometries. We report here for the first time, analytical expressions for correcting residual stresses in *internal* holes (e.g. inside surface of a bolt hole). For practical geometries of interest, FE based correction procedure has been recommended in the literature. The sensitivity of such a correction procedure to the choice of material properties and stress gradients is investigated here. We also present case studies of split-sleeve cold expanded hole and multi-level shot-peened plate as practical applications of FE based corrections.

1 Introduction

X-Ray diffraction has evolved as one of the most practical methods to measure surface residual stresses. The method is regularly used to measure sub-surface stresses by removing thin surface layers by electro-polishing. When such layer removal is performed, the measured stress needs to be corrected for the stress relaxation and redistribution that occurs because of layer removal. The underlying principles of mechanics for this method are described by Francois et.al. [1]. Most standards on XRD measurements (e.g. SAE HS-784 [2]) cite analytical solutions derived and published in 1958 by Moore and Evans [3] as a recommended correction for simple geometries. We have extended these corrections by developing and implementing analytical solutions for internal holes – a geometry of interest in aircraft engine applications.

Further, when the geometry is not simple and/or only a portion of the material is removed instead of a full layer, these analytical solutions are not valid. Finite element based correction methodology has been previously published by Hornbach et. al. [4] and Lambda Research [5]. It has been claimed that purely geometry dependent correction factors can be developed for typical stress distributions of interest. It is not obvious if and how these corrections are sensitive to the choice of material properties and stress levels, as well as gradients. In this work, we will evaluate this assumption and demonstrate that while the concept works very well with linear elastic finite element analysis, the correction matrix is sensitive to material model, as well as qualitative and quantitative nature of residual stress distribution.

It will be shown that the developed transfer functions depend on geometry, material property and stress distribution. We will show results for such corrections on specimens with split sleeve cold expanded (SSCE) holes and a flat plate with different levels of shot-peening. It will be demonstrated that given the asymmetric stress distribution along the circumference of the holes and the large depth of high compressive stresses in case of SSCE processes, the correction procedure must account for plasticity. In the case of shot-peening

alone, since the corrections are small relative to the magnitude of stresses, a simpler approach with linear analysis may suffice.

For the case of a flat plate with multiple alternatively peened zones, it is shown that removing sufficiently small regions of material from a particular shot-peened region does not disturb residual stresses over the rest of the plate and thus an efficient testing plan can be developed that enables testing of various shot-peening conditions with minimal number of specimens.

This paper is organized as follows. Section 2 presents the analytical expressions for correcting residual stresses in internal holes. A finite element based correction method utilizing numerical transfer functions (published previously [4, 5]) is summarized and illustrated in section 3. Section 4 discusses the assumptions and limitations underlying the FE based transfer function approach. Sections 5 and 6 describe applications of the FE based transfer function approach to split sleeve cold expanded holes and a multi shot peened plate respectively. A discussion of the results and some concluding remarks complete the paper.

2 Analytical Correction for Internal holes with rotationally symmetric stresses

In the present section, we derive stress corrections for internal holes with rotationally symmetric stresses. Initially, we consider stress relaxations in a hollow circular cylinder in which material layers on the inner surface are removed. We note that stresses on isolated circular holes in most geometries can often be modeled using a hollow circular cylinder (see figure) in which $R \gg R_1$. Following the approach in [3], removal of a thin outer shell of thickness dr in a hollow circular cylinder with a residual stress distribution

$$-\frac{\sigma_{\theta m}(r)}{r} dr,$$

results in removal of a small outward force $\frac{\sigma_{\theta m}(r)}{r}$ from each square unit of inner surface of the remaining cylinder. Employing the known solution to the stress problem of a hollow cylinder subject to uniform internal pressure, we obtain the following relaxations in the stress components on the inner surface:

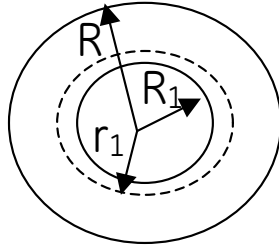


Figure 1. Internal Hole Layer removal: Schematic representation

$$\text{r direction stress} = -\frac{\sigma_{\theta m}(r)}{r} \frac{r^2}{R^2 - r^2} \left(1 - \frac{R^2}{r_1^2} \right) dr \quad (1)$$

$$\text{\theta direction stress} = -\frac{\sigma_{\theta m}(r)}{r} \frac{r^2}{R^2 - r^2} \left(1 + \frac{R^2}{r_1^2} \right) dr \quad (2)$$

$$\text{z direction stress} = -\sigma_{zm}(r) \frac{2\pi dr}{\pi(R^2 - r^2)} dr \quad (3)$$

Where $\sigma_{\theta m}(r)$ and $\sigma_{zm}(r)$ are measured stresses at radius r . The corrected stresses can be obtained by adding equations 1 through 3 to the measured stresses.

r direction stress =

$$\sigma_r^{act}(r_1) = - \left(1 - \frac{R^2}{r_1^2} \right) \int_{R_1}^{r_1} \frac{r \sigma_{\theta m}(r)}{R^2 - r^2} dr \quad (4)$$

θ direction stress =

$$\sigma_{\theta}^{act}(r_1) = \sigma_{\theta m}(r_1) - \left(1 + \frac{R^2}{r_1^2} \right) \int_{R_1}^{r_1} \frac{r \sigma_{\theta m}(r)}{R^2 - r^2} dr = \sigma_{\theta m}(r_1) + \frac{r_1^2 + R^2}{r_1^2 - R^2} \sigma_r^{act}(r_1) \quad (5)$$

z direction stress =

$$\sigma_z^{act}(r_1) = \sigma_{zm}(r_1) - 2 \int_{R_1}^{r_1} \frac{r \sigma_{zm}(r)}{R^2 - r^2} dr \quad (6)$$

As mentioned previously, we take the limit $R \rightarrow \infty$ in order to get expressions for the case when $R \gg R_1$:

$$\sigma_r^{act}(r_1)|_{R \rightarrow \infty} = \frac{1}{r^2} \int_{R_1}^{r_1} r \sigma_{\theta m}(r) dr$$

r direction stress = (7)

$$\sigma_{\theta}^{act}(r_1)|_{R \rightarrow \infty} = \sigma_{\theta m}(r_1) + \sigma_r^{act}(r_1)|_{R \rightarrow \infty} \quad (8)$$

$$\sigma_z^{act}(r_1)|_{R \rightarrow \infty} = \sigma_{zm}(r_1) \quad (9)$$

3 FE based Transfer Function

A practical approach for correcting measured residual stresses was first reported by Lambda Research [5]. They developed a methodology based on FE simulations of the layer removal process. An efficient way of modeling layer removal in a commercial FE program like Ansys is to employ its element death option ('ekill' command in Ansys APDL). This essentially sets the stiffness of selected elements to a very small value (default $\sim 10E-6$ of Young's modulus of underlying material). If the actual residual stress distribution in a part can be introduced in a FE model (e.g. by process simulation or some appropriate temperature distribution), then the FE based transfer function approach – as reported in [5] - can be employed. The basic concept of such an approach is discussed below for completeness and to facilitate discussion of assumptions and limitations in the following section.

Let us consider a plate with some near surface residual stress distribution. We introduce a residual stress field as shown by the blue line in the chart in Figure 1. We generate the Measured-FE curve by removing layers using the 'ekill' command. The XRD measurement is non-destructive in nature and thus one gets the true stress value (needs to be corrected for gradient correction due to finite depth of penetration X ray beam – please refer to Section 7.3 in SAE HS-784 for details). However, once a surface layer of material is removed for subsurface measurements, the residual stress that is measured at any given depth (e.g. 108.55 ksi at 1 mil) is different from what it was prior to the layer removal (e.g. -100.96 ksi). Thus diagonal entries (green and bold) are expected measured values (as obtained from FE layer removal simulation). Now, as Lambda's report explains, it will be useful if, for a given geometry, the correction at a particular layer removal step can be normalized with respect to the measured value. This will allow us to run only one FE run with a fictitious residual stress profile, and generate a transfer function that can be used for correcting measured values on that geometry.

The column under the heading 3 mil denotes stresses obtained from FE at depths from 3 mil to 8 mil after 3 mils were removed. The next table shows $\Delta\sigma$ which is the change in stress at a given depth due to removal of another layer. e.g. Change of 2.68 ksi is obtained at layer 4 (at 4 mil) when second layer from 1 to 2 mils is removed. Now, this value of 2.68 is divided by measured value at 2 mils (-125 ksi) to get a coefficient in the transfer function (a lower triangular matrix) as shown in the third table – thus giving an entry of 0.0214 at the intersection of row 4 and column 2. Another example for entry K_{63} is shown in the Figure 2. Then, once the transfer function is formed, the total correction required at each layer is computed by a simple matrix – vector multiplication. Note that if we use the transfer function on the measured values from FE we will get back the original stress distribution. But, more importantly, it is hypothesized that this transfer function remains unaltered on any other stress distribution for the same geometry and layer removal sequence. We evaluate this hypothesis in detail in the next section.

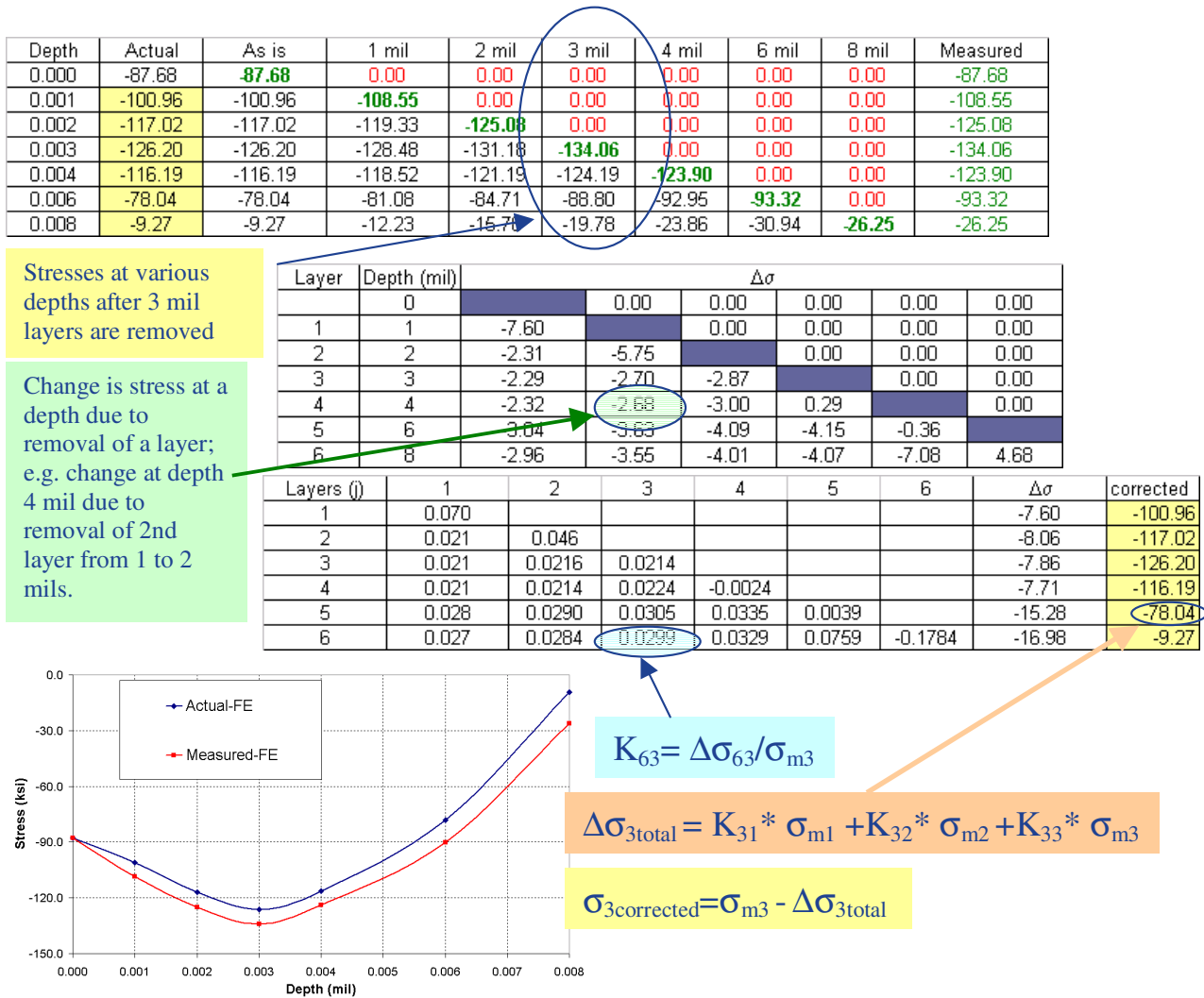


Figure 2. FE Based transfer function: how does it work?

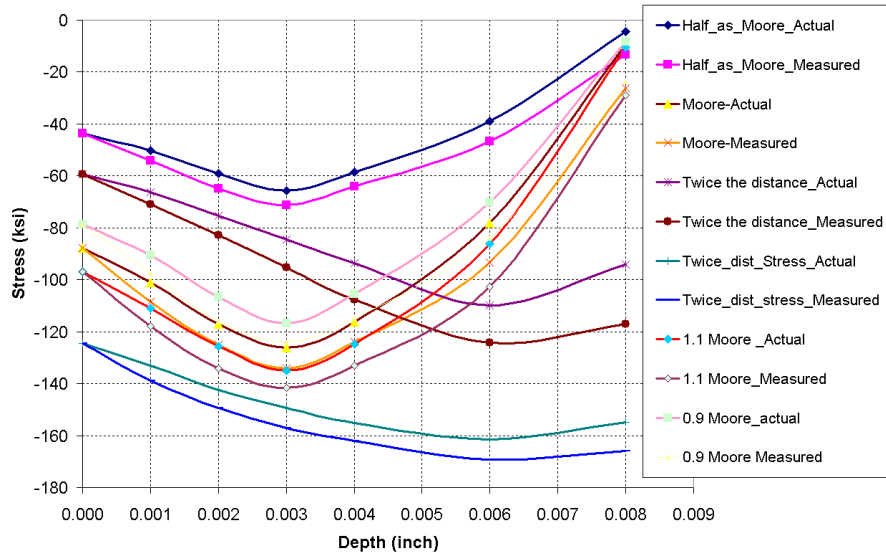


Figure 3. Actual and Measured stress profiles for a range of surface stress distributions

4 FE based Transfer Function: Assumptions and limitations

The key advantage of using the FE based transfer function approach as described in the previous section is its simplicity. Also, since the entries in transfer function are normalized with the measured stresses, it is intuitively conceivable that the function works well when the measured values are offset by a certain magnitude. However, there is no information in the transfer function about the gradient of stress that is removed in a single layer removal step. We investigated the transferability of entries in the transfer function matrix for several different stress profiles. In the Appendix, we provide an evidence of how even the diagonal entries in the transfer function would depend on the stress profile. In the remainder of this section, we take a more practical approach and evaluate the percentage changes that are expected for a range of profiles and how they impact the “corrected” stresses themselves.

We investigated a range of surface stress distributions and generated transfer functions for each of them as described above. Note that we used the same geometry (thick plate with 3D FEM in Ansys) and removed the same layers in each step. We used Moore-Evans’ example (Figure 13 in reference [3]) to develop a baseline case and then vary the stresses such that there is a uniform shift of +/- 10% (1.1 Moore and 0.9 Moore in Figure 3) and also a case where the stress magnitudes are only half of that reported by Moore-Evans. Two additional cases are investigated – the first case has the same maximum stress as the Moore-Evans example but the maximum stress occurs at twice the Moore-Evans depth; the second case has a maximum stress of about 1.3 times that of the Moore Evans example which occurs at twice the Moore-Evans depth. Figure 4 illustrates the percentage change in the transfer function entries relative to the base line case. Note that all the analyses shown in Figure 3 are run assuming elastic-plastic material properties.

1.3	1	2	3	4	5	6
1	-73.77%	#DIV/0!	#DIV/0!	#DIV/0!	#DIV/0!	#DIV/0!
2	-68.98%	-70.71%	#DIV/0!	#DIV/0!	#DIV/0!	#DIV/0!
3	-74.65%	-76.91%	-76.52%	#DIV/0!	#DIV/0!	#DIV/0!
4	-68.49%	-70.24%	-71.74%	-44.39%	#DIV/0!	#DIV/0!
5	-43.84%	-47.27%	-53.54%	-66.85%	-189.11%	#DIV/0!
6	25.01%	18.06%	10.72%	0.54%	-10.99%	7.70%
1.1	1	2	3	4	5	6
1	-15.9%	#DIV/0!	#DIV/0!	#DIV/0!	#DIV/0!	#DIV/0!
2	2.9%	0.2%	#DIV/0!	#DIV/0!	#DIV/0!	#DIV/0!
3	-22.6%	-24.0%	-23.1%	#DIV/0!	#DIV/0!	#DIV/0!
4	-0.2%	1.3%	-9.4%	-78.6%	#DIV/0!	#DIV/0!
5	2.9%	1.3%	2.3%	-0.8%	-33.0%	#DIV/0!
6	3.0%	1.4%	2.4%	-0.8%	-1.6%	0.0%

Higher compression

2X depth; 1.3	1	2	3	4	5	6
1	-41.50%	#DIV/0!	#DIV/0!	#DIV/0!	#DIV/0!	#DIV/0!
2	-5.51%	-41.39%	#DIV/0!	#DIV/0!	#DIV/0!	#DIV/0!
3	-23.90%	-28.24%	-4.98%	#DIV/0!	#DIV/0!	#DIV/0!
4	-41.66%	-53.65%	-57.87%	-709.62%	#DIV/0!	#DIV/0!
5	-61.84%	-65.32%	-68.76%	-75.63%	187.53%	#DIV/0!
6	-54.03%	-63.86%	-67.70%	-72.40%	-77.59%	-106.07%

Baseline case

Layers (j)	1	2	3	4	5	6
1	0.070					
2	0.021	0.046				
3	0.021	0.0216	0.0214			
4	0.021	0.0214	0.0224	-0.0024		
5	0.028	0.0290	0.0305	0.0335	0.0039	
6	0.027	0.0284	0.0299	0.0329	0.0759	-0.1784

0.9	1	2	3	4	5	6
1	0.00%	#DIV/0!	Lower compression	#DIV/0!	#DIV/0!	#DIV/0!
2	-0.01%	-0.01%	#DIV/0!	#DIV/0!	#DIV/0!	#DIV/0!
3	0.00%	0.00%	0.00%	#DIV/0!	#DIV/0!	#DIV/0!
4	-0.01%	0.00%	0.00%	0.00%	#DIV/0!	#DIV/0!
5	0.00%	0.00%	0.00%	0.00%	0.00%	#DIV/0!
6	0.00%	0.00%	0.00%	0.00%	0.00%	0.00%
0.5	1	2	3	4	5	6
1	-0.93%	#DIV/0!	#DIV/0!	#DIV/0!	#DIV/0!	#DIV/0!
2	35.47%	35.57%	#DIV/0!	#DIV/0!	#DIV/0!	#DIV/0!
3	34.99%	32.68%	35.76%	#DIV/0!	#DIV/0!	#DIV/0!
4	30.82%	32.35%	35.44%	10.99%	#DIV/0!	#DIV/0!
5	-2.69%	-4.90%	-2.70%	1.10%	24.98%	#DIV/0!
6	-2.63%	-5.01%	-2.82%	0.99%	1.22%	0.00%

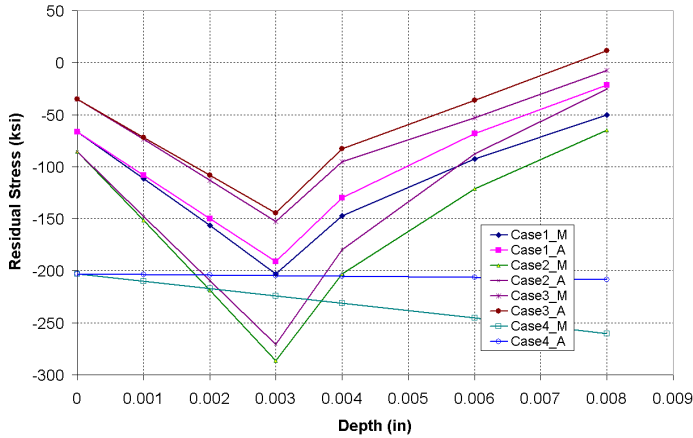
2 X depth	1	2	3	4	5	6
1	-5.40%	#DIV/0!	#DIV/0!	#DIV/0!	#DIV/0!	#DIV/0!
2	61.76%	32.69%	#DIV/0!	#DIV/0!	#DIV/0!	#DIV/0!
3	60.21%	56.90%	164.68%	#DIV/0!	#DIV/0!	#DIV/0!
4	54.40%	55.43%	48.40%	-2370.36%	#DIV/0!	#DIV/0!
5	9.39%	-19.52%	-23.40%	-30.51%	1072.05%	#DIV/0!
6	11.39%	8.59%	3.78%	-4.92%	-20.67%	-121.58%

Higher depth (Stretched profile)

Figure 4. Comparison of transfer function change due to profiles (Baseline case shows actual entries in the transfer function, all other cases, show percent change in a entry relative to baseline)

As noticed from Figure 4, the transfer function entries change significantly with different profiles. Note that for high compressive stress values the correction is only 5-10% of the measured value and thus, difference in correction matrix results in "inaccurate" correction, however, the corrected stresses are still within 5% of actual stresses (or the stresses calculated using appropriate transfer function).

Since the nonlinear properties affect the change in transfer function in addition to change in stress profile, we also repeated the study by running analyses with linear material properties on a limited set of profiles. As shown in Figure 5, the percentage change in transfer function with profiles is significantly reduced.



Constant stress

Case 4					
19.60%	#DIV/0!	#DIV/0!	#DIV/0!	#DIV/0!	#DIV/0!
19.00%	19.41%	#DIV/0!	#DIV/0!	#DIV/0!	#DIV/0!
22.20%	18.77%	16.79%	#DIV/0!	#DIV/0!	#DIV/0!
18.63%	14.84%	12.34%	-16.84%	#DIV/0!	#DIV/0!
14.85%	11.03%	8.24%	-19.27%	-28.84%	#DIV/0!
12.06%	7.85%	5.24%	-21.69%	-30.42%	-37.91%

Case 1	1	2	3	4	5	6
1	0.026					
2	0.026	0.025399				
3	0.025	0.0253	0.0254			
4	0.025	0.0258	0.0262	0.0350		
5	0.025	0.0259	0.0265	0.0353	0.0779	
6	0.025	0.0258	0.0265	0.0355	0.0782	0.0875

Case1 * 1.5

Case 2					
-4.56%	#DIV/0!	#DIV/0!	#DIV/0!	#DIV/0!	#DIV/0!
-5.00%	-5.01%	#DIV/0!	#DIV/0!	#DIV/0!	#DIV/0!
-6.60%	-6.13%	-5.54%	#DIV/0!	#DIV/0!	#DIV/0!
-4.59%	-4.04%	-3.70%	-2.25%	#DIV/0!	#DIV/0!
-2.95%	-2.36%	-1.99%	-0.37%	1.86%	#DIV/0!
-2.21%	-1.56%	-1.20%	0.46%	2.68%	0.37%

Case1 * 0.73

Case 3					
-7.86%	#DIV/0!	#DIV/0!	#DIV/0!	#DIV/0!	#DIV/0!
-6.32%	-3.45%	#DIV/0!	#DIV/0!	#DIV/0!	#DIV/0!
-6.04%	-2.34%	0.05%	#DIV/0!	#DIV/0!	#DIV/0!
-6.26%	-2.42%	-0.65%	11.16%	#DIV/0!	#DIV/0!
-6.87%	-3.08%	-1.29%	10.20%	8.86%	#DIV/0!
-6.76%	-2.94%	-1.23%	10.38%	8.81%	193.32%

Figure 5. Comparison of transfer function change due to profiles when running elastic-only analysis.

5 Application to Cold-expanded Hole

It is often desirable to perform split sleeve cold expansion on holes to improve their fatigue life. It is also known that split sleeve cold expanded holes can have deep compressive residual stresses. FE model of the SSCE process was developed in Ansys to understand extent and magnitude of compressive stresses given a fixed percentage of expansion. Figure 6 shows a FE model of such a hole in a plate of Nickel based super alloy and the resulting compressive stresses in the hoop direction around the hole. The hoop stress is plotted along the path AB as shown in the FE mesh. Actual stress refers to stress obtained from FE analysis of the SSCE process. At the end of the SSCE load step, we select a few rows of elements around the inner perimeter of the hole and simulate layer removal on the inner surface by using the ekill command in Ansys. For example, elements up to 7.5 mil thickness in radial direction and remove that layer. Then, the hoop stress at the new free surface is designated as "Predicted Measurements". This is because a stress of approximately 180ksi in compression would be measured if one were to remove 7.5 mil layer from the hole and then measure the surface stress using XRD. Note that the actual stress at that point was only about -170 ksi; thus a significant correction will be required to obtain the original stress field. Using stress distributions after SSCE and during step-wise layer removal, FE based transfer function can be developed for correction of measured stresses. Note that FE analyses of the SSCE process can be expensive and actual measured stresses – even from the same nominal SSCE expansion – may not match exactly with "predicted measurements". In this situation we investigate how reasonable it is to continue to use the transfer function based on "nominal" conditions for a somewhat different stress profile. The easiest numerical exercise is to generate SSCE profiles for 2 more expansion percentages – one being 2.5% less than Nominal percent expansion (e.g. if Nominal expansion is 1%, one can run FE with expansion of 0.975%) and another with 25% less expansion (e.g. for 1% nominal, it will be 0.75%). Then, we remove layers in FE and calculate "predicted measured" values. Now, we correct these predicted measured values using the transfer function developed using nominal expansion conditions. As noted from Figure 7, for Nominal -2.5% case, the difference in "corrected" and actual stresses is within 1 ksi, whereas for Nominal -25%, the difference can be 10-15 ksi. The engineers should decide if errors of 10-15 ksi are important enough to justify running FE analyses to capture the actual profile and generate a transfer function that is more accurate for their applications.

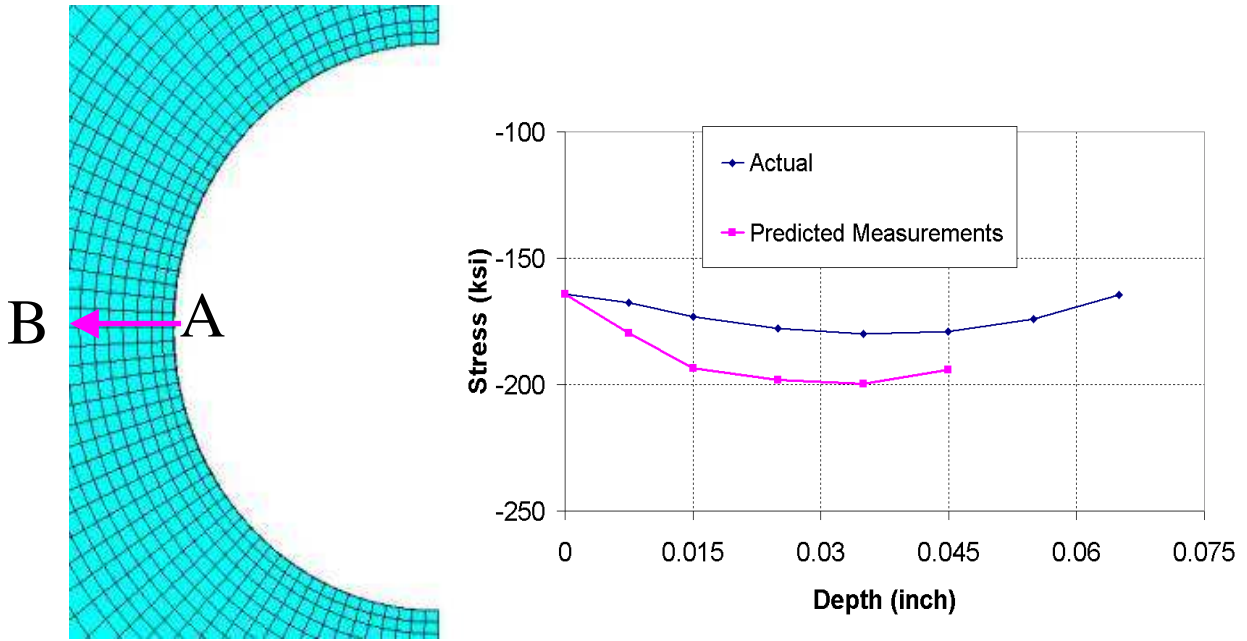


Figure 6. SSCE Hole: Deep residual stress profile and thus higher corrections required

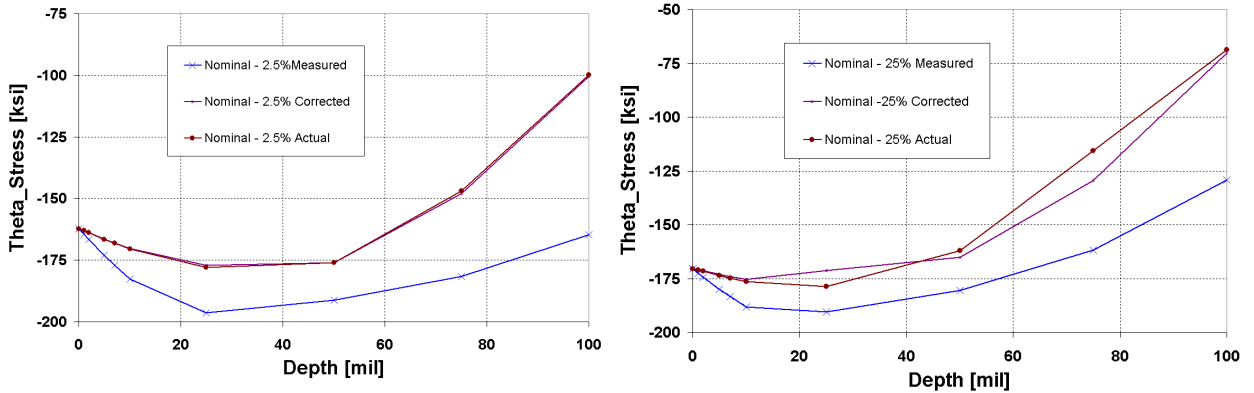


Figure 7. How does a transfer function developed for Nominal SSCE expansion work with 0.25% and 25% change in Percent expansion.

6 Multi-shot-peened Plate

Often it is desirable to evaluate residual stresses introduced by different levels of shot-peening. Given the cost of materials, processing and simplicity, it is desirable to shot-peen different portions of the same plate with different intensities and coverage. The X-Ray measurements of such plates will involve removing pockets instead of full layers. Also, given that the Moore-Evan's solutions are strictly valid for removing a constant stress over the entire layer, we investigated how FE modeling can be used to understand this problem. One other key issue is that of whether the stress state in a lightly peened region can get disturbed

when material from such a region is removed layer-by-layer to create a 200 mil square pocket. In Figure 8, we designate four regions as A, B, C and D. Figure 9 shows FE stress contours when 4 layers of pocket (200 mil square) are removed from region A, and when 4 layers of pockets in A, B and C are removed. The contours qualitatively demonstrate that the stress state in regions B, C, and D remain essentially unchanged as a pocket in region A is removed. In Figure 10, we show quantitatively how (a) region B stresses are unaffected when a pocket is removed in steps of 0.002 inch in region A and (b) region C stresses are unaffected when pocket in A completely removed and pocket in B is incrementally removed in steps of 0.002 inches.

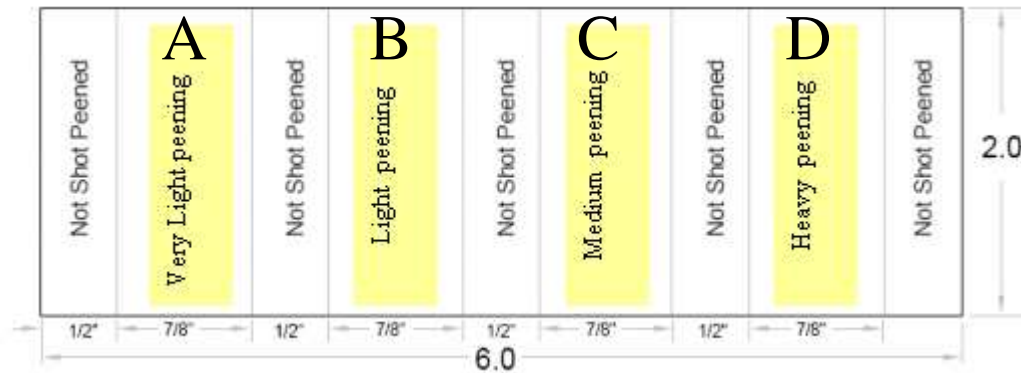


Figure 8. Plate geometry

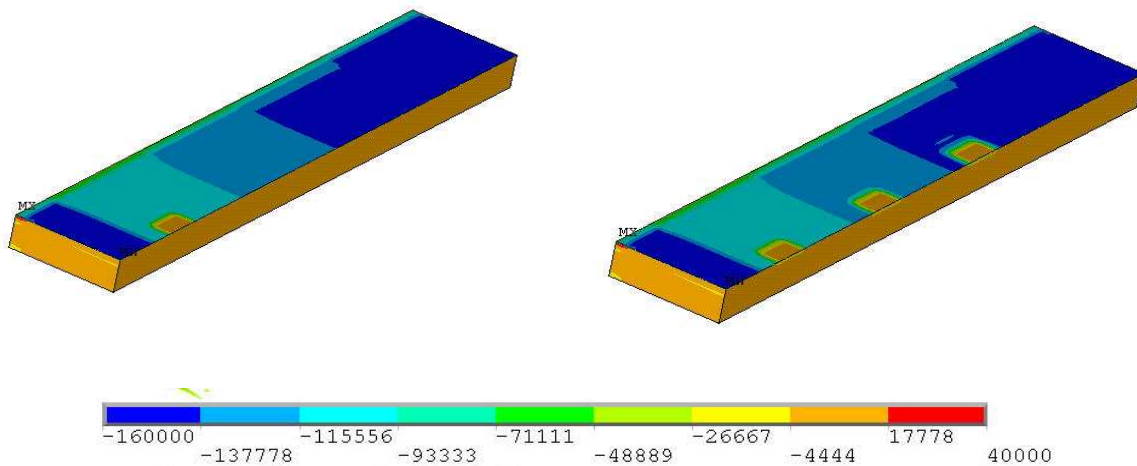


Figure 9. Illustration of half model and 200 mil pocket removal

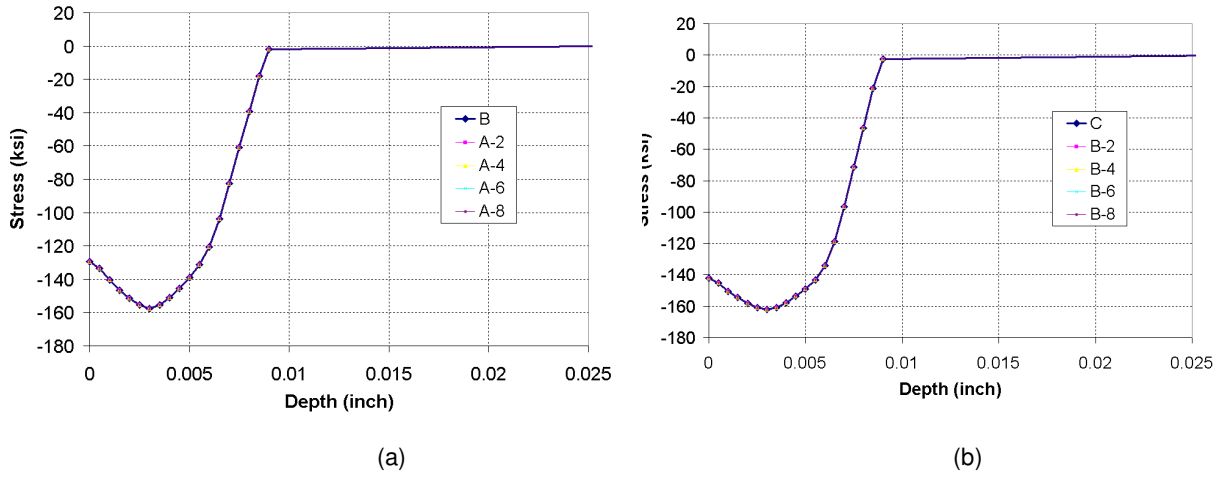


Figure 10. Illustration of how stresses in adjacent regions are not affected by pocket removals

7 Conclusions and discussion

The following remarks are in order:

1. Although the FE based transfer function methodology has been found to work well for many practical engineering applications, it is demonstrated that the definition of the transfer function may not be universal in nature. The dependence of the transfer function on the nature of the stress profile, and the choice of the FE analysis (elastic-only or elastic-plastic) is demonstrated in this paper in a quantitative manner. It is also shown analytically how the elements of the correction matrix can be complex functions of the actual stress profile (see Appendix).
2. We report, for the first time, analytical corrections for layer removal on internal holes.
3. Since the FE based transfer function can depend on the actual stress profile, it is proposed that a more generalized approach be formulated wherein a transfer function is developed based on a *set of residual stress profiles* that function as a basis set capable of spanning other possible stress profiles. For example, the information contained in various pairs of measured and actual stresses in Figure 3 can be used to develop a transfer function that can predict actual stresses given an arbitrary stress profile. Such a tool would enable *a priori* FE runs from a broad range of residual stress profiles of interest to accurately predict the corrected stress profile in a case for which no FE run was made.

APPENDIX

Analytical evaluation of transferability of the correction matrix to changes in the actual stress profile

We analytically investigate the transferability of the correction matrix to changes in the actual stress profile by considering the specific case of axial stresses in a solid circular cylinder for which the corrected stresses have been expressed in terms of the measured stresses in [3]. Consider a solid circular cylinder with axisymmetric stresses with initial radius, R and actual stress in the axial direction denoted by $\sigma_z(r)$.

Approach

1. Start with the Moore-Evans solution for $\sigma_z(r)$ given in terms of $\sigma_{zm}(r)$
2. Invert this solution to get $\sigma_{zm}(r)$ in terms of $\sigma_z(r)$

3. Express the diagonal entries of the correction matrix in terms of $\sigma_{zm}(r)$ and $\sigma_z(r)$

$$\frac{\sigma_{zm}(r_1) - \sigma_z(r_1)}{\sigma_{zm}(r_1)}$$

For e.g., First row, first column element = where (R-r1) is the thickness of the first removed layer.

4. Check if this expression changes upon changing $\sigma_z(r)$.

a. Moore-Evans Solution:

$$\sigma_z(r) = \sigma_{zm}(r) - 2 \int_r^R \frac{\sigma_{zm}(x)}{x} dx \quad (\text{A-1})$$

b. Inverting this solution: Differentiating the equation:

$$\frac{d\sigma_z}{dr} = \frac{d\sigma_{zm}}{dr} + 2 \frac{d\sigma_{zm}(r)}{r} \quad (\text{A-2})$$

We can solve for $\sigma_{zm}(r)$ given $\sigma_z(r)$ with the known condition that $\sigma_{zm}(R) = \sigma_z(R)$

This is a first order linear ODE for which one can use the following standard solution approach:

Integrating factor, $u(r) = e^{\int \frac{2}{r} dr} = e^{2 \ln r} = r^2$

$$\sigma_{zm}(r) = \frac{1}{r^2} \left[\int_R^r r^2 \left(\frac{d\sigma_z}{dr} \right) dr + const \right] \quad (\text{A-3})$$

Using the condition $\sigma_{zm}(R) = \sigma_z(R)$

$$\sigma_{zm}(r) = \frac{R^2}{r^2} \sigma_z(R) + \frac{1}{r^2} \int_R^r r^2 \left(\frac{d\sigma_z}{dr} \right) dr \quad (\text{A-4})$$

It is straightforward to verify that differentiating equation 11 gives equation 9.

c. Assume that a thickness of (R-r1) is removed at the first removal step. From equation 11 we have

$$\sigma_{zm}(r_1) = \frac{R^2}{r_1^2} \sigma_z(R) + \frac{1}{r_1^2} \int_R^{r_1} r^2 \left(\frac{d\sigma_z}{dr} \right) dr \quad (\text{A-5})$$

The first row, first column element of correction matrix is given by $\frac{\sigma_{zm}(r_1) - \sigma_z(r_1)}{\sigma_{zm}(r_1)}$. In the following, we assume a linear $\sigma_z(r)$ across the depth of (R - r1) [in which case the FE and Moore-Evans relaxations can be shown to coincide].

Let $\sigma_z(r) = a + br$ and $\sigma_z(R) = a + bR$

$$\frac{d\sigma_z}{dr} = b$$

We have

$$\sigma_{zm}(r_1) = \frac{R^2}{r_1^2} (a + bR) + \frac{1}{r_1^2} \left[b \int_R^{r_1} r^2 dr \right]$$

$$\sigma_{zm}(r_1) = \frac{R^2}{r_1^2} (a + bR) + \frac{b}{3r_1^2} \left[(r_1^3 - R^3) \right]$$

(A-6)

From step c we can conclude that the first row and first column element of the correction matrix depends on a and b. For a different stress profile with different values of parameters a and b, this element would change and is not independent of profile. This approach can be easily extended to some other Moore-Evans cases as well.

References

1. Francois, M., Convert, F., Lu, J. et. al., Handbook of Measurement of Residual Stresses, Society of Experimental Mechanics, Inc., Ed. Jian Lu, 71-132, 1996
2. SAE International, Residual Stress Measurement by X-Ray Diffraction, HS-784, 77-84, 2003
3. Moore, M.G. and Evans, W.P., SAE Transactions, Vol. 66, 340-345, 1958
4. Hornbach, D.J., Prevey, P.S., and Mason, P.W., In Proceedings of the First International Conference on Induction Hardened Gears and Critical Components, Indianapolis, IN, Gear Research Institute, 69-76, 1995
5. Lambda Research, Diffraction Notes, No.17, 1996